Frenkel and Charge-Transfer Excitations in Donor–acceptor Complexes from Many-Body Green's Functions Theory

Björn Baumeier,[†],[*] Denis Andrienko,[†] and Michael Rohlfing[‡]

[†]Max Planck Institute for Polymer Research, Ackermannweg 10, 55128 Mainz, Germany
[‡]Department of Physics, University of Osnabrück, Barbarastr. 12, 49069 Osnabrück, Germany

ABSTRACT: Excited states of donor–acceptor dimers are studied using many-body Green's functions theory within the *GW* approximation and the Bethe–Salpeter equation. For a series of prototypical small-molecule based pairs, this method predicts energies of local Frenkel and intermolecular charge-transfer excitations with the accuracy of tens of meV. Application to larger systems is possible and allowed us to analyze energy levels and binding energies of excitons in representative dimers of dicyanovinyl-substituted quarterthiophene and fullerene, a donor–acceptor pair used in state of the art organic solar cells. In these dimers, the transition from Frenkel to charge transfer excitons is endothermic and the binding energy of charge transfer excitons is still of the order of 1.5−2 eV. Hence, even such an accurate dimer-based description does not yield internal energetics favorable for the generation of free charges either by thermal energy or an external electric field. These results confirm that, for qualitative predictions of solar cell functionality, accounting for the explicit molecular environment is as important as the accurate knowledge of internal dimer energies.

I. INTRODUCTION

Converting molecular photoexcitations to free charges is at the heart of functionality of all photovoltaic devices.[1,2] In organic solar cells, strong binding energies (of the order of eV) of Frenkel excitons (FE) localized on single molecules cannot be overcome by thermal energy only. Consequently, a donor–acceptor (DA) heterostructure is required to drive charge separation, which results in charge-transfer (CT) states with a hole localized on a donor and electron on an acceptor of a DA complex. CT states are more delocalized than FE and thus have smaller binding energies. It is generally assumed that they split either due to external field[3−5] or by using the excess energy of the FE→CT transition, which helps escaping the Coulomb attraction between the charges.[4,5] Experimentally, evidence for either model is difficult to obtain since these processes can be probed only indirectly.

In this situation, insight from theoretical modeling into the electronic processes occurring at DA interfaces can help to resolve such open questions. It has been shown that polarizable environments, either formed by a polar solvent[6,7] or the presence of polarizable molecular aggregates,[8] strongly influence the nature of electronic (excited) states and thereby the conversion processes of photoexcitations. Considerable effort is therefore directed at combinations of quantum-mechanical and molecular-mechanics modeling approaches,[9] in which a cluster of molecules treated at first-principles level is embedded into an environment that is described, for example, by a polarizable force field. For reliable predictions from such schemes, both the quantum and classical parts need to be sufficiently accurate and not limited to model structures.

For the quantum-mechanical description of excitations in molecular DA structures in such approaches, we evaluate the potential of using many-body Green's functions theory within the GW approximation and the Bethe–Salpeter equation (GW-BSE).[10−12] This method has already been shown to provide quantitatively accurate *ab initio* predictions of excited states of crystals,[13,14] polymers,[15] small inorganic and organic molecules,[16,17] and small-molecule organic semiconductors.[18,19] Here, we pay special attention to the simultaneous treatment of localized and charge-transfer excitations in donor–acceptor dimers.

To this end, we first employ many-body Green's functions theory to study the excited states of small bimolecular donor–acceptor complexes consisting of aromatic donors (D = benzene, toluene, *o*-xylene, and naphthalene) and a tetracyanoethylene (TCNE) acceptor, and we analyze their excitations in terms of the local or charge-transfer character. For this set of dimers, accurate experimental energies of charge-transfer excitations are available from gas-phase absorption measurements[20] and reliable calculations,[21−23] which serve as a reference for the assessment of the accuracy of the method.

We then apply the method to representative dimers of terminally substituted quarterthiophene (DCV4T) with (C60-Ih)[5,6]fullerene (C_{60}), a donor–acceptor combination used in state of the art small-molecule-based organic solar cells.[24−26] Herein, we demonstrate that the treatment of complexes of sizes relevant for organic devices is possible and allows to analyze the relative internal energy alignment of Frenkel and charge-transfer excitations as well as the reduction in electron–hole binding energy as a function of the molecular arrangement.

II. METHODOLOGY

Here, we briefly summarize the key points of many-body Green's functions theory within the *GW* approximation and the Bethe–Salpeter equation. The procedure and implementation is identical to that described in more detail in refs 19, 27, and 28. Many-body Green's functions theory is used to treat

charged (electron removal/addition) and neutral (optical) excitations. This approach is based on a set of Green's functions equations of motion, containing both the nonlocal, energy-dependent electronic self-energy Σ and the electron–hole interaction leading to the formation of excitons, described by the Bethe–Salpeter equation (BSE). The first step of the procedure consists of the calculation of molecular orbitals and energies on density-functional theory (DFT) level as solutions of the Kohn–Sham equations

$$\left\{ -\frac{\hbar^2}{2m}\nabla^2 + V_{ECP}(\mathbf{r}) + V_H(\mathbf{r}) + V_{xc}(\mathbf{r}) \right\}\psi_n^{KS}(\mathbf{r})$$
$$= E_n^{KS}\psi_n^{KS}(\mathbf{r}) \tag{1}$$

Here, V_{ECP} is an effective-core potential (ECP), V_H the Hartree potential, and V_{xc} the exchange-correlation potential. Single-particle excitations are then obtained within the *GW* approximation of many-body Green's functions theory, as introduced by Hedin and Lundqvist,[10] by substitution of the energy-dependent self-energy operator $\Sigma(\mathbf{r},\mathbf{r}',E)$ for the DFT exchange-correlation potential, giving rise to the quasiparticle equations

$$\left\{ -\frac{\hbar^2}{2m}\nabla^2 + V_{ECP}(\mathbf{r}) + V_H(\mathbf{r}) \right\}\psi_n^{QP}(\mathbf{r})$$
$$+ \int \Sigma(\mathbf{r}, \mathbf{r}', E_n^{QP})\psi_n^{QP}(\mathbf{r}')d\mathbf{r}' = E_n^{QP}\psi_n^{QP}(\mathbf{r}) \tag{2}$$

The self-energy operator is evaluated as

$$\Sigma(\mathbf{r}, \mathbf{r}', E) = \frac{i}{2\pi}\int e^{-i\omega0^+} G(\mathbf{r}, \mathbf{r}', E - \omega)W(\mathbf{r}, \mathbf{r}', \omega)d\omega \tag{3}$$

where

$$G(\mathbf{r}, \mathbf{r}', \omega) = \sum_n \frac{\psi_n(\mathbf{r})\psi_n^*(\mathbf{r}')}{\omega - E_n + i0^+\text{sgn}(E_n - \mu)} \tag{4}$$

is the one-body Green's function in quasiparticle (QP) approximation and

$$W = \varepsilon^{-1}v \tag{5}$$

is the dynamically screened Coulomb interaction, comprising the dielectric function ε, computed within the random-phase approximation, and the bare Coulomb interaction v. Herein, both G and W are determined from ground-state Kohn–Sham wave functions and energies. If not treated carefully, the self-energy and the resulting QP energies may deviate from self-consistent results, since fundamental gap is underestimated within DFT. We use an iterative procedure, in which W is calculated only once, using a Kohn–Sham spectrum that is scissors-shifted so that the resulting QP gap is matched. The resulting QP energy levels are iterated several times, updating the Green's function of eq 4 and thus the self-energy, until convergence is reached. A one-shot G_0W_0 calculation from Kohn–Sham energies may differ from our results by up to several 0.1 eV. Note that our (limited) self-consistency treatment does change the QP structure of eq 4 (due to satellite structures or other consequences of a self-consistent spectral shape of $G(\omega)$).

To treat coupled excitations of an electron and a hole, for example, as the result of photoexcitation, it is required to go beyond the effective one-particle picture. Instead, an electron–hole state can be described as

$$\Phi(\mathbf{r}_e, \mathbf{r}_h) = \sum_\alpha^{occ}\sum_\beta^{virt}[A_{\alpha\beta}\psi_\beta(\mathbf{r}_e)\psi_\alpha^*(\mathbf{r}_h) + B_{\alpha\beta}\psi_\alpha(\mathbf{r}_e)\psi_\beta^*(\mathbf{r}_h)] \tag{6}$$

where α and β denote the single-particle occupied and virtual orbitals, respectively, and $A_{\alpha\beta}$ and $B_{\alpha\beta}$ are resonant (occ.→virt.) and antiresonant (virt.→occ.) electron–hole amplitudes. These amplitudes can be obtained by solving a non-Hermitian eigenvalue problem known as the generalized Bethe–Salpeter equation

$$\begin{pmatrix} R & C \\ -C^* & -R^* \end{pmatrix}\begin{pmatrix} A \\ B \end{pmatrix} = \Omega\begin{pmatrix} A \\ B \end{pmatrix} \tag{7}$$

in which we defined the free interlevel transition energy $D = E_{virt}^{QP} - E_{occ}^{QP}$, $R = D + \eta K^{R,x} + K^{R,d}$ is the resonant (and $-R^*$ the antiresonant) Hamiltonian of the transition, while $C = \eta K^{C,x} + K^{C,d}$ is the coupling term between resonant and antiresonant transitions (with $\eta = 2(0)$ for singlet (triplet) transitions). $K^{j,x}$ and $K^{j,d}$ (with $j = R,C$) are the bare exchange and screened direct terms of the electron–hole interaction kernel, respectively. We include dynamic screening effects in the electron–hole interaction kernel perturbatively (see refs 19 and 27 for details). Finally, Ω is the transition energy of the optical excitation.

When the resonant–antiresonant coupling terms C are much smaller than R, the resonant and antiresonant parts of the full BSE (eq 7) decouple. In this Tamm–Dancoff approximation (TDA) the electron–hole wave function is given by $\Phi_S(\mathbf{r}_e,\mathbf{r}_h) = \sum_\alpha^{occ}\sum_\beta^{virt} A_{\alpha\beta}\psi_\beta(\mathbf{r}_e)\psi^*_\alpha(\mathbf{r}_h)$, and a standard Hermitian eigenvalue problem (of smaller dimension than eq 7) needs to be solved. For a single DCV4T molecule, we showed that the use of the TDA overestimates $\pi-\pi$ transition energies by 0.2 eV but yields correct character of the excitations.[19]

For practical calculations according to the *GW*-BSE method, we perform single-point Kohn–Sham calculations using a modified[29] version of the Gaussian03 package,[30] the PBE functional, Stuttgart/Dresden effective core potentials,[31] and the associated basis sets that are augmented by additional polarization functions[32] of *d* symmetry. The use of ECPs offers a computational advantage as the wave functions entering the *GW* procedure are smooth close to the nuclei and do not require strongly localized basis functions, keeping the numerical effort tractable. We confirmed that the Kohn–Sham energies obtained from ECP-based calculations do not deviate significantly from all-electron results. The actual *GW*-BSE calculations are performed using a code that is specifically optimized for molecular systems.[19,27,28] Therein, the quantities occurring in the *GW* self-energy operator and the electron–hole interaction in the BSE are expressed in terms of atom-centered Gaussian basis functions of the form $\chi_{ijk}(\mathbf{r}) = A_{ijk}x^iy^jz^k$ $\exp(-\alpha\mathbf{r}^2)$. We include orbitals of s, p, d, and s* symmetry with the decay constants α (in a.u.) 0.20, 0.67, and 3.0 for N and S, 0.25, 0.90, 3.0 for C, and 0.4 and 1.5 for H atoms, yielding converged excitation energies. Further technical details can be found refs 19, 17, and 28.

III. EXCITATIONS IN AROMATIC DONOR–TCNE COMPLEXES

Optimized ground state geometries of the dimer configuration of the four aromatic donors with the TCNE acceptor molecule

are taken from the Supporting Information of ref 21. In the lower panel of Figure 1, we show the evolution of excitation
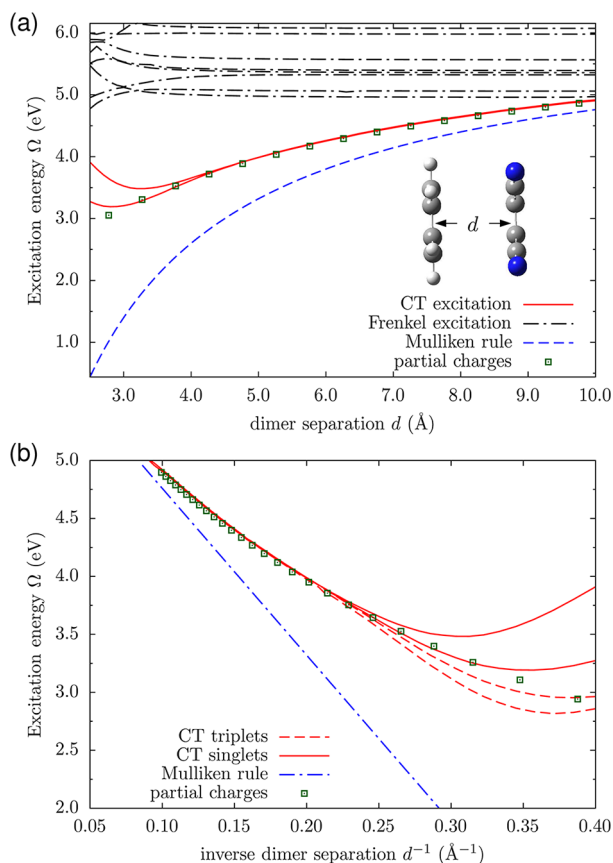
Figure 1. (a) Frenkel (dash-dotted) and charge-transfer (solid) excitation energies (in eV) of a π-stacked benzene−TCNE dimer as a function of intermolecular separation d (in Å). The dashed line is an estimation of the energy of a CT exciton according to Mulliken's rule, while boxes indicate the results of a classical estimate based on atomic partial charges, according to eq 8. (b) Excitation energies of CT singlets (solid) and CT triplets as a function of $1/d$.

spectrum of a π-stacked dimer consisting of benzene and TCNE with increasing separation d between the molecules. We take into account 384 levels (37 occupied, 347 virtual states) for the calculation of the polarizability within the random-phase approximation, and determine quasiparticle corrections for the 74 lowest energy states, which we include in the possible transitions within the BSE. One can clearly distinguish two types of excitations. The spectrum above 5.0 eV is dominated by local excitations, whose energy is practically independent of the dimer configuration with the exception of separations smaller than typical van-der-Waals distances due to short-range interactions of the involved single-particle orbitals. In contrast, the two (due to the 2-fold degeneracy of the highest occupied molecular orbital of benzene) lowest excitation energies increase with larger separation of donor and acceptor and asymptotically approach the quasiparticle gap E_{HL} = 6.2 eV of a dimer with infinite separation, or the charge-separated state. Such a distance dependence is characteristic for charge-transfer excitations dominated by Coulomb interactions. A classical description of this dependence using a bare Coulomb interaction between integer point charges for electron and hole as $\Omega_{CT} = IP(D) - EA(A) - d^{-1}$, shown as the dashed line

in Figure 1 (Mulliken rule), clearly underestimates the energies resulting from our *GW*-BSE calculations.

The observed disagreement between our result and the classical estimate using the Mulliken rule for separations larger than typical van der Waals distances can, in principle, be due to the nonlocality of charge distribution and screening $\sim \varepsilon^{-1}(\mathbf{r}, \mathbf{r}')$, which is present in the direct term of the electron−hole interaction kernel of the Bethe−Salpeter equation. To identify the origin of the deviation in the benzene−TCNE dimer, we have calculated atomic partial charges for the benzene cation (adding up to +1) and TCNE anion (adding up to −1) from a distributed multipole analysis,[33] and estimate the CT excitation energy classically according to

$$\Omega_{CT} = IP(D) - EA(A) + \sum_{i \in D} \sum_{j \in A} \frac{q_i q_j}{|\mathbf{r}_i - \mathbf{r}_j|} \tag{8}$$

The resulting energies as a function of distance are shown as boxes in Figure 1 and reproduce mid- to long-range distance-dependence of the lowest singlet charge-transfer excitation as obtained by *GW*-BSE. This indicates that the deviation of the Mulliken rule is due to the explicit molecular charge distribution, that is well reproduced by atomic partial charges, but not by integer point charges assigned to the center of mass of donor and acceptor molecules, respectively. Polarization effects are negligible in this case since the molecular polarizabilities of donor cation and acceptor anion are only on the order of 1 Å^3 in the stacking direction of the dimer.

For distances shorter than ∼4 Å, explicit structural details of the single-particle wave functions $\psi_\alpha(\mathbf{r}_h)$ and $\psi_\beta(\mathbf{r}_e)$ enter both the exchange and direct term of the electron−hole interaction kernel. By comparing triplet to singlet CT energies in Figure 1b, one can see that the exchange term (only present for singlets) affects the short-range excitation energies more strongly than the screened direct term.

A quantitative comparison of the *GW*-BSE energies of charge-transfer excitations to the time-dependent density-functional theory (TDDFT) with range-separated functionals[21] and experimental measurements in the gas phase[20] is given in Table 1. We identify CT excitations at energies of 3.52, 3.31,

Table 1. Excitation Energies (in eV) and Oscillator Strength of Charge-Transfer Excitations in Optimized D-TCNE Dimers using TDDFT with Generic (E^{gen}) and Optimized (E^{opt}) Range-Separated Hybrid Functionals,[21] *GW*-BSE, and Experiment[20]

	TDDFT			*GW*-BSE		exp.	
D	E^{gen}	E^{opt}	f	E	f	E	f
benzene	4.4	3.8	0.03	3.52	0.04	3.59	0.02
toluene	4.0	3.4	0.03	3.31	0.05	3.36	0.03
o-xylene	3.7	3.0	0.01	3.13	0.05	3.15	0.05
naphthalene	3.3	2.7	∼0	2.56	∼0	2.60	0.01

3.13, and 2.56 eV, which is in excellent agreement with the experimental data of 3.59, 3.36, 3.15, and 2.60 eV. This also agrees well with the results of ref 23 and the TDDFT calculations (E^{opt}) with a range-separated hybrid functional, in which the range-separation has been optimized using a first-principles procedure. In contrast, generic range-separated functionals (E^{gen}) substantially overestimate the experimental energies, while results from standard semilocal and hybrid functionals not only severely underestimate them (e.g.,

resulting as 1.4 eV using PBE and 2.0 eV using B3LYP in benzene-TCNE) but also fail to exhibit the long-range Coulomb behavior. Our *GW*-BSE results for the dimers do not depend on the specific choice of a functional during the initial DFT step, emphasizing that method intrinsically contains all required many-body effects that are needed to treat local and CT excitations on equal footing. We should also note that, in our implementation, a calculation of the benzene−TCNE spectrum including the ground-state DFT run takes ca. 10 min on a single node of a desktop computer.

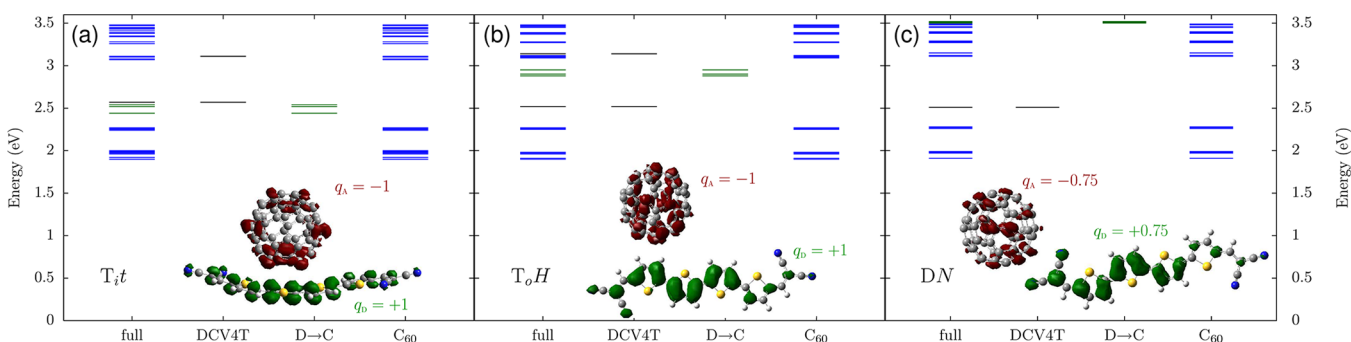## IV. DONOR−ACCEPTOR COMPLEXES IN ORGANIC SOLAR CELLS

Having confirmed that *GW*-BSE provides reliable predictions of energies of local and charge-transfer excitations in molecular dimers, we now consider dimers of a dicyanovinyl-substituted quarterthiophene donor and a C_{60} acceptor which are used in small-molecule based organic solar cells.[25,34]

Starting from several initial configurations (see Figure 2), ground state geometries are optimized within DFT using
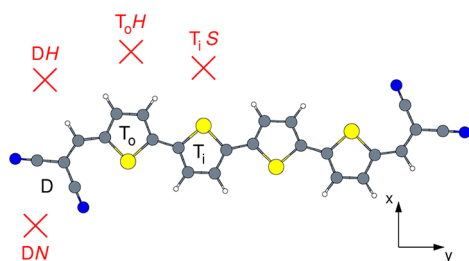
Figure 2. Initial configurations of DCV4T:C_{60} dimers. Top view including definition of D, T_o, and T_i subunits of DCV4T. In DN, DH, T_nH (hydrogen face of T_n), and T_nS (sulfur face of T_n) configurations, the center of mass of the fullerene is positioned within the *x-y*-plane in direction indicated by the crosses at 4 Å distance of closest approach to DCV4T. In Dt, T_ot, and T_it configurations (not shown) the C_{60} is positioned in *z*-direction above the respective subunits.

TURBOMOLE,[35] employing the def2-TZVP basis set with the B3LYP hybrid functional and an empirical dispersion correction.[36] We find seven stable configurations. The minimum energy structure (T_it) corresponds to the arrangement of the fullerene on top of one of the inner thiophene units of the oligomer backbone (see inset of Figure 3a), maximizing their π−π interaction.

The full singlet excitation spectrum of the minimum energy configuration (T_it)[37] shown in Figure 3a consists of local excitations on DCV4T and C_{60}, as well as CT transitions between the two. We decompose the total spectra in terms of the individual contributions according to the effective charge $q_S^{h(e),i} = \Sigma_{\alpha\beta}|A_{\alpha\beta}^S|^2 p_{\alpha(\beta)}^i$ localized on either monomer i = D,C, where $p_{\alpha(\beta)}^i$ are monomer-resolved Mulliken populations of the single-particle orbitals.[38]

The full spectra are dominated by (optically inactive) FE on the fullerene acceptor. In particular, the 15 lowest singlet excitations in the energy range from 1.95 to 2.38 eV are transitions between the C_{60} frontier orbitals. The calculated lowest singlet excitation energy in the dimers is nearly identical to that in a single fullerene, since its geometry is not perturbed and no mixing with donor orbitals is taking place. Quantitatively, the value of 1.95 eV is in close agreement to experimental data of 1.9 eV.[39] The lowest FE of DCV4T can be found at about 2.5 eV, which is ca. 0.1 eV higher than the energy obtained for a single DCV4T molecule mainly due to its distorted geometry in the presence of the fullerene. One can clearly identify a set of three donor−acceptor (D → C) CT states with energies about 0.1 eV below that of the optically excited donor exciton and an effectively transferred charge of 1e. Interestingly, the lowest of these CT excitations, that is, the one with the strongest π−π interaction, shows an oscillator strength of f = 0.06. This indicates the possibility of a direct photoexcitation of the CT state at about a tenth of the absorption into the DCV4T exciton.

In general, we find for the other DCV4T:C_{60} dimer structures that the energy of the CT states in relation to that of the donor FE is very sensitive to the arrangement of donor and acceptor molecules. In Figure 3b, we show for comparison the decomposed excitation spectrum of the T_oH configuration, in which the fullerene acceptor is adjacent to the hydrogen atoms of the outer thiophene units of the backbone and its center-of-mass is in plane with DCV4T. Here, the energies of FE on donor and acceptor are practically identical to those in the T_it arrangement, while the CT states are found about 0.2 eV above the lowest excitation of DCV4T, as the interaction of the two π-systems decreases.

When the fullerene is close to the nitrogen atoms of one of the terminal dicyanovinyl groups of DCV4T, as shown in the inset of Figure 3c, no CT excitation with energy close to that of the donor FE can be identified. The proximity of the C_{60} to this strongly electronegative group leads to an increased spatial separation of the π-systems involved in the formation of the CT

Figure 3. Singlet excitation energies (in eV) of sample DCV4T:C_{60} dimers. The spectra are decomposed into contributions from FE on DCV4T and C_{60}, respectively, and CT excitations from DCV4T to C_{60}. Insets show the difference electron density distribution isovalue $[\pm 0.001]$ e/Å³ and the effective charges on donor and acceptor for a selected CT state.

states. Also, the local electrostatic environment of two units with acceptor character is unfavorable for the formation of a charge-transfer exciton close in energy to the donor FE so that the CT energy is as high as 3.5 eV.

Also for these dimers, we determine atomic partial charges for a C_{60} anion and DCV4T cation and estimate the respective CT excitation energy classically according to eq 8 . The obtained energies of 2.76 eV for $T_i t$, 3.15 eV for $T_o H$, and 3.82 eV for DN, respectively, overestimate the *GW*-BSE results by roughly 0.3 eV. These deviations can be traced back to more intricate interactions between the involved π-systems. Both C_{60} and the donor molecule (in particular along the π-conjugated backbone) are strongly polarizable. Intradimer polarization affects the distribution of electronic densities on the molecules, which is clearly visible in the hole density distribution on DCV4T shown in the insets of Figure 3 . Note also that, for the DN arrangement, only a charge 0.75e is transferred from donor to acceptor, in contrast to the integer charge transfer found in the other two configurations. Both, polarization effects and noninteger charge transfer cannot be described accurately using eq 8.

To relate the results to the solar cell functionality we will first analyze the difference of CT and Frenkel excitation energies, $\Delta\Omega = \Omega^{CT} - \Omega^{FE}$. $\Delta\Omega$ is an internal contribution to the driving force (site energy difference) entering the rate of the phonon-induced conversion of Frenkel to charge-transfer excitations. In our case, $\Delta\Omega$, which is shown in Figure 4 for all dimers, varies between $+1$ and -0.1 eV, which implies that at a realistic interface there will be DA pairs with both positive (uphill) and

negative (downhill) driving forces. Interestingly, the only dimer with the negative driving force is the minimum energy structure ($T_i t$). Here, the DCV4T molecule bends around the fullerene, which increases the energy of the FE localized on the DCV4T molecule. On the other hand, strong $\pi-\pi$ interaction between DCV4T and fullerene increases the binding energy of the CT state, which overall results in a (small) negative driving force. Such negative $\Delta\Omega$ can potentially boost the rate of the phonon-induced conversion of Frenkel to charge-transfer excitations. The other configurations have rather large positive driving force of 0.4 eV, on average. Experimental estimation of $\Delta\Omega$ from EA(A)−EA(D) is of the order of -0.2 eV[25] and hence provides an excess energy favoring creation of a hot CT state.

After a CT state is created, the relevant quantity for the charge-separation process is the exciton binding energy, E_B^{CT}. Within *GW*-BSE, we quantify the binding energy of the exciton by the expectation value of the electron−hole interaction kernel, $E_B = \langle \Phi_S | K^{e-h} | \Phi_S \rangle$, where

$$K_{e-h} = \begin{pmatrix} R - D & C \\ -C^* & -(R-D)^* \end{pmatrix}$$

as used in eq 7. The CT state is expected to have smaller binding energy than FE. The reduction in binding energy, $\Delta E_B = E_B^{CT} - E_B^D < 0$, shown in Figure 4, indeed confirms this statement. However, the actual reduction of the FE binding is rather small, of the order of -0.2 eV for energetically favorable transitions (the biggest loss of binding energy is found for those configurations with large $\Delta\Omega$, but these processes have very small rates in a dimer-only picture). The remaining binding energy of the CT state is still of the order of 1.5−2 eV, which is impossible to overcome thermally or via external field. The fact that our calculations on isolated dimers cannot reproduce the experimental excitation and binding energies is not a shortcoming of *GW*-BSE. It is known that a polarizable environment can strongly influence the energetics and, in particular, lead to an additional stabilization of electronic (excited) states.[6−9] Qualitatively, it can be expected that the CT excitation has, due to the more separated charges, a higher dipole moment than the FE and should, therefore, be more strongly stabilized. For a quantitative estimate of such *external* effects, often implicit solvation models are employed, but it has been observed that those underestimate the effect of a solvent on charge-transfer states[21,40] by several tenths of an eV. In amorphous solids such as a vapor-deposited donor−acceptor blend used in the active layer of organic solar cells, it is crucial to account for explicit morphological detail,[41] which is often achieved by a combination of quantum- and molecular modeling.[9] Further differences between our calculations and the experimental observations could arise, for example, due to polaronic stabilization of both bound and separated charges.

We finally comment on the conversion from photoexcited singlet donor FE to the donor triplet population via a "ping-pong" effect.[42] Here, a singlet energy transfer occurs between DCV4T (2.5 eV) and C_{60} (≤ 2.2 eV), where the nonvanishing intersystem crossing allows for singlet−triplet conversion to the C_{60} triplet (≥ 1.5 eV) followed by the back transfer to the DCV4T (1.1 eV) triplet. Hence, from the point of view of energetics and without accounting for environmental effects, such a loss mechanism is always possible.
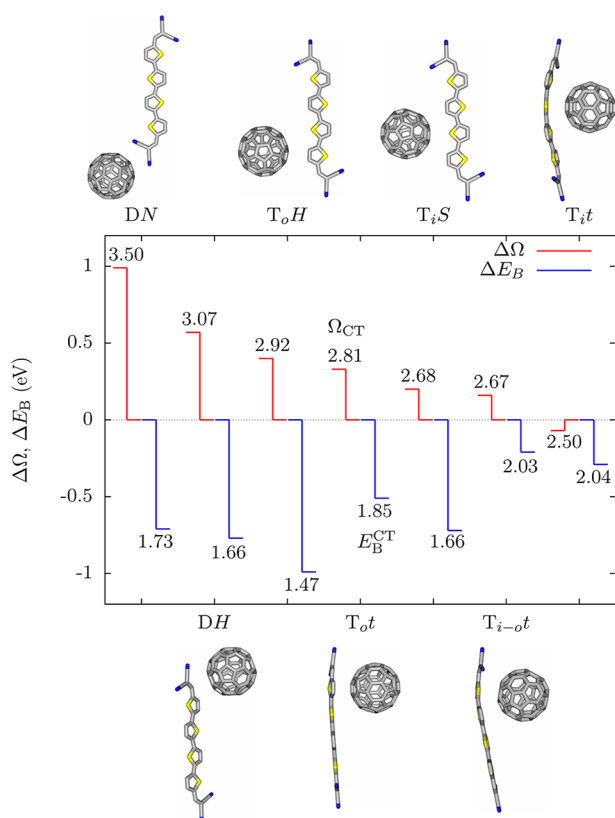
Figure 4. Difference in excitation ($\Delta\Omega = \Omega_{CT} - \Omega_D$) and binding ($\Delta E_B = E_B^{CT} - E_B^D$) energies (in eV) of CT and donor excitations. The numbers are the average excitation (Ω_{CT}) and the average binding (E_B^{CT}) energies of the CT state.

V. SUMMARY

To summarize, the use of *GW*-BSE provides a reliable prediction of the character and energetics of both Frenkel and charge-transfer excitations in molecular donor−acceptor dimers. A quantitative relation of these *internal* energies to the processes occurring at a donor−acceptor junctions in an organic solar cell, however, has to additionally account for effects of the explicit polarizable environment formed by the local electric fields of the surrounding molecules. In fact, such *external* effects cannot be considered at required accuracy using implicit solvation[21] or lattice models. Instead, explicit morphological details[41] must be accounted for by combining accurate internal energies obtained using *GW*-BSE with classical polarizable force field methods for external interactions. This work is in progress.

■ AUTHOR INFORMATION

Corresponding Author
*Email: baumeier@mpip-mainz.mpg.de.

Notes
The authors declare no competing financial interest.

■ ACKNOWLEDGMENTS

■ REFERENCES

(1) Li, G.; Zhu, R.; Yang, Y. *Nat. Photonics* **2012**, *6*, 153−161.
(2) Bakulin, A. A.; Rao, A.; Pavelyev, V. G.; van Loosdrecht, P. H. M.; Pshenichnikov, M. S.; Niedzialek, D.; Cornil, J.; Beljonne, D.; Friend, R. H. *Science* **2012**, *335*, 1340−1344.
(3) Peumans, P.; Forrest, S. R. *Chem. Phys. Lett.* **2004**, *398*, 27−31.
(4) Ohkita, H.; Cook, S.; Astuti, Y.; Duffy, W.; Tierney, S.; Zhang, W.; Heeney, M.; McCulloch, I.; Nelson, J.; Bradley, D. D. C.; Durrant, J. R. *J. Am. Chem. Soc.* **2008**, *130*, 3030−3042.
(5) Liedtke, M.; Sperlich, A.; Kraus, H.; Baumann, A.; Deibel, C.; Wirix, M. J. M.; Loos, J.; Cardona, C. M.; Dyakonov, V. *J. Am. Chem. Soc.* **2011**, *133*, 9088−9094.
(6) Carbonera, D.; Di Valentin, M.; Corvaja, C.; Agostini, G.; Giacometti, G.; Liddell, P. A.; Kuciauskas, D.; Moore, A. L.; Moore, T. A.; Gust, D. *J. Am. Chem. Soc.* **1998**, *120*, 4398−4405.
(7) Baruah, T.; Pederson, M. R. *J. Chem. Theory Comput.* **2009**, *5*, 834−843.
(8) Beljonne, D.; Cornil, J.; Muccioli, L.; Zannoni, C.; Brédas, J.; Castet, F. *Chem. Mater.* **2010**, *23*, 591−609.
(9) Yost, S. R.; Wang, L.; Van Voorhis, T. *J. Phys. Chem. C* **2011**, *115*, 14431−14436.
(10) Hedin, L.; Lundqvist, S. *Solid State Physics: Advances in Research and Application*; Academix Press: New York, 1969; Vol. 23, pp 1−181.
(11) Rohlfing, M.; Louie, S. G. *Phys. Rev. B* **2000**, *62*, 4927.
(12) Onida, G.; Reining, L.; Rubio, A. *Rev. Mod. Phys.* **2002**, *74*, 601.
(13) Albrecht, S.; Reining, L.; Del Sole, R.; Onida, G. *Phys. Rev. Lett.* **1998**, *80*, 4510.
(14) Shirley, E. L. *Phys. Rev. Lett.* **1998**, *80*, 794.
(15) Artacho, E.; Rohlfing, M.; Côté, M.; Haynes, P. D.; Needs, R. J.; Molteni, C. *Phys. Rev. Lett.* **2004**, *93*, 116401.
(16) Rohlfing, M.; Louie, S. G. *Phys. Rev. Lett.* **1998**, *80*, 3320.
(17) Tiago, M. L.; Chelikowsky, J. R. *Phys. Rev. B* **2006**, *73*, 205334.
(18) Blase, X.; Attaccalite, C.; Olevano, V. *Phys. Rev. B* **2011**, *83*, 115103.
(19) Baumeier, B.; Andrienko, D.; Ma, Y.; Rohlfing, M. *J. Chem. Theory Comput.* **2012**, *8*, 997−1002.
(20) Hanazaki, I. *J. Phys. Chem.* **1972**, *76*, 1982−1989.
(21) Stein, T.; Kronik, L.; Baer, R. *J. Am. Chem. Soc.* **2009**, *131*, 2818−2820.
(22) Blase, X.; Attaccalite, C. *Appl. Phys. Lett.* **2011**, *99*, 171909.
(23) Faber, C.; Duchemin, I.; Deutsch, T.; Attaccalite, C.; Olevano, V.; Blase, X. *J. Mater. Sci.* **2012**, 1−10.
(24) Riede, M.; Mueller, T.; Tress, W.; Schueppel, R.; Leo, K. *Nanotechnology* **2008**, *19*, 424001.
(25) Fitzner, R.; Reinold, E.; Mishra, A.; Mena-Osteritz, E.; Ziehlke, H.; Körner, C.; Leo, K.; Riede, M.; Weil, M.; Tsaryova, O.; Weiß, A.; Uhrich, C.; Pfeiffer, M.; Bäuerle, P. *Adv. Funct. Mater.* **2011**, *21*, 897−910.
(26) Meiss, J.; Menke, T.; Leo, K.; Uhrich, C.; Gnehr, W.; Sonntag, S.; Pfeiffer, M.; Riede, M. *Appl. Phys. Lett.* **2011**, *99*, 043301.
(27) Ma, Y.; Rohlfing, M.; Molteni, C. *Phys. Rev. B* **2009**, *80*, 241405.
(28) Ma, Y.; Rohlfing, M.; Molteni, C. *J. Chem. Theory. Comput.* **2010**, *6*, 257−265.
(29) The source code of Gaussian03 was modified to output the matrix elements of the exchange-correlation potential in the atomic orbital basis, needed to calculate the matrix $\langle n|V_{xc}|m \rangle$, where $|n\rangle$ and $|m\rangle$ are Kohn−Sham wave functions, as input for the *GW*-BSE steps.
(30) Frisch, M. J.; Trucks, G. W.; Schlegel, H. B.; Scuseria, G. E.; Robb, M. A.; Cheeseman, J. R.; Montgomery, J. A. Jr.; Vreven, T.; Kudin, K. N.; Burant, J. C.; Millam, J. M.; Iyengar, S. S.; Tomasi, J.; Barone, V.; Mennucci, B.; Cossi, M.; Scalmani, G.; Rega, N.; Petersson, G. A.; Nakatsuji, H.; Hada, M.; Ehara, M.; Toyota, K.; Fukuda, R.; Hasegawa, J.; Ishida, M.; Nakajima, T.; Honda, Y.; Kitao, O.; Nakai, H.; Klene, M.; Li, X.; Knox, J. E.; Hratchian, H. P.; Cross, J. B.; Bakken, V.; Adamo, C.; Jaramillo, J.; Gomperts, R.; Stratmann, R. E.; Yazyev, O.; Austin, A. J.; Cammi, R.; Pomelli, C.; Ochterski, J. W.; Ayala, P. Y.; Morokuma, K.; Voth, G. A.; Salvador, P.; Dannenberg, J. J.; Zakrzewski, V. G.; Dapprich, S.; Daniels, A. D.; Strain, M. C.; Farkas, O.; Malick, D. K.; Rabuck, A. D.; Raghavachari, K.; Foresman, J. B.; Ortiz, J. V.; Cui, Q.; Baboul, A. G.; Clifford, S.; Cioslowski, J.; Stefanov, B. B.; Liu, G.; Liashenko, A.; Piskorz, P.; Komaromi, I.; Martin, R. L.; Fox, D. J.; Keith, T.; Al-Laham, M. A.; Peng, C. Y.; Nanayakkara, A.; Challacombe, M.; Gill, P. M. W.; Johnson, B.; Chen, W.; Wong, M. W.; Gonzalez, C.; Pople, J. A. *Gaussian 03*, Revision B. 05; Gaussian, Inc.: Wallingford, CT, 2004.
(31) Bergner, A.; Dolg, M.; Küchle, W.; Stoll, H.; Preuß, H. *Mol. Phys.* **1993**, *80*, 1431−1441.
(32) Krishnan, R.; Binkley, J. S.; Seeger, R.; Pople, J. A. *J. Chem. Phys.* **1980**, *72*, 650.
(33) Stone, A. J. *J. Chem. Theory Comput.* **2005**, *1*, 1128−1132.
(34) Fitzner, R.; Elschner, C.; Weil, M.; Uhrich, C.; Körner, C.; Riede, M.; Leo, K.; Pfeiffer, M.; Reinold, E.; Mena-Osteritz, E.; Bäuerle, P. *Adv. Mater.* **2012**, *24*, 675−680.
(35) *TURBOMOLE V6.3* 2011; (accessed May 1, 2012).
(36) Grimme, S. *J. Comput. Chem.* **2006**, *27*, 1787−1799.
(37) The polarizability was calculated using 195 occupied and 1825 virtual states in the random-phase approximation. Quasiparticle corrections are calculated for the 390 lowest-energy states, and 30 occupied and 30 virtual states are considered in the Bethe−Salpeter equation.
(38) The excitations are classified based on a TDA caluculation (due to proper normalization of the excited state wave functions) as local excitations on DCV4T ($q_S^{h,D}, q_S^{e,D} > 0.7$) and C_{60} ($q_S^{h,C}, q_S^{e,C} > 0.7$), and the CT excitations from DCV4T to C_{60} ($q_S^{h,D}, q_S^{e,D} > 0.7$) and from C_{60} to DCV4T ($q_S^{h,C}, q_S^{e,D} > 0.7$).
(39) van den Heuvel, D. J.; van den Berg, G. J. B.; Groenen, E. J. J.; Schmidt, J.; Holleman, I.; Meijer, G. *J. Phys. Chem.* **1995**, *99*, 11644−11649.
(40) Liao, M.; Lu, Y.; Parker, V. D.; Scheiner, S. *J. Phys. Chem. A* **2003**, *107*, 8939−8948.
(41) Rühle, V.; Lukyanov, A.; May, F.; Schrader, M.; Vehoff, T.; Kirkpatrick, J.; Baumeier, B.; Andrienko, D. *J. Chem. Theory Comput.* **2011**, *7*, 3335−3345.
(42) Schueppel, R.; Schmidt, K.; Uhrich, C.; Schulze, K.; Wynands, D.; Brédas, J. L.; Brier, E.; Reinold, E.; Bu, H.; Baeuerle, P.; Maennig, B.; Pfeiffer, M.; Leo, K. *Phys. Rev. B* **2008**, *77*, 085311.